Applied Catalysis B: Environmental 152–153 (2014) 342–351

Contents lists available at ScienceDirect

Applied Catalysis B: Environmental

journal homepage: www.elsevier.com/locate/apcatb

Degradation of bezafibrate in wastewater by catalytic ozonation with cobalt doped red mud: Efficiency, intermediates and toxicity

Huanan Li[a], Bingbing Xu[b], Fei Qi[a,*], Dezhi Sun[a], Zhonglin Chen[c,**]

[a] Beijing Key Lab for Source Control Technology of Water Pollution, College of Environmental Science and Engineering, Beijing Forestry University, Beijing 100083, PR China
[b] State Key Laboratory of Environmental Criteria and Risk Assessment, Chinese Research Academy of Environmental Sciences, Beijing 100012, PR China
[c] State Key Laboratory of Urban Water Resource and Environment, Harbin Institute of Technology, Harbin 150090, PR China

ARTICLE INFO

Article history:
Received 28 September 2013
Received in revised form 26 January 2014
Accepted 28 January 2014
Available online 4 February 2014

Keywords:
Bezafibrate
Catalytic ozonation
Co/red mud
Hydroxyl radical

ABSTRACT

The bezafibrate (BZF) degradation and mineralization performances of a red mud (RM) catalyst doped with cobalt (i.e. Co/RM) during the ozonation reaction have been evaluated experimentally. The purposes of this study were to study the performance reaction mechanism and intermediate. In a next stage of our study also economic evaluations for a large scale application will be considered. Results of this study showed that catalytic ozonation using Co/RM not only led to the successful degradation of BZF, but also mineralized the corresponding intermediates, in ultrapure water as well as the effluent of wastewater. Detoxification was also achieved in this reaction process. The surface and structure properties of Co/RM were characterized by several analytical methods. The leaching of toxic heavy metal from the catalyst used in this process was very low, with the heterogeneous reaction dominating the decomposition of BZF, which made the reuse of the catalyst highly feasible. The enhanced generation of hydroxyl radical was critical to the success of the catalytic activity. Furthermore, 22 of the intermediates generated during this process were identified and several degradation pathways were proposed

1. Introduction

A variety of different studies have been reported in recent years regarding the occurrence of a large number of residual pharmaceutical (PhAC) agents in the aquatic environment [1], and there are concerns that the presence of these residues in secondary effluents could have an adverse impact on the aquatic organisms living in the receiving waters as well as having a long-term effect on aquatic ecosystems and human health if the reclaimed water is returned to the water supply [2]. Furthermore, it is well known that conventional wastewater treatment plants are poorly equipped to handle this particular problem [3,4].

Bezafibrate (BZF, *p*-[4-[chlorobenzoylamino-ethyl]-phenoxy]-b-methylpropionic acid) is a fibrate drug that is currently used extensively as a lipid regulating agent [5]. Recent investigations revealed that BZF was present in a variety of different aquatic systems throughout the developed world, including the influent/effluent waters of sewage treatment plants (STPs), because of the large consumption of BZF in these countries [6]. The bioaccumulation and bio-magnification of BZF could be potentially very harmful to the aquatic environment because of possible mixture toxicity, synergistic and additives effects [7]. Nanofiltration and reverse osmosis appear to be effective methods for the removal of BZF from water, although the BZF is invariably transferred to the concentrate and not degraded [8]. A number of advanced oxidation processes (AOPs) have also been used for the degradation of BZF, such as ozonation [9,10], UV irradiation [6], pulse radiolysis [11], UV/H_2O_2 [6], UV/TiO_2 [5] and photo-Fenton [12]. Furthermore, the intermediates and reaction mechanisms associated with the degradation of BZF via the ozonation and UV/TiO_2 pathways have been identified by gas chromatography–mass spectrometry (GC–MS) and liquid chromatography–mass spectrometry (LC–MS) [5]. The reaction mechanism for the degradation of BZF by the UV/H_2O_2, however, remains unknown and may be different from these two processes [6].

Catalytic ozonation using a solid catalyst has been the subject of increasing levels of interest from the drinking water and wastewater treatment industries [13,14]. There are several key advantages to this technology, including its ability to (1) enhance the reaction rate of the sole ozonation process (SOP); (2) improve the mineralization process; and (3) reduce the yield of the intermediates and the toxicity of the effluent. A variety of different catalysts are commonly used for this process, including activated carbon [15,16],

* Corresponding author. Tel.: +86 10 62336615; fax: +86 10 62336596.
** Corresponding author.
E-mail addresses: qifei@bjfu.edu.cn (F. Qi), zhonglinchen@163.com (Z. Chen).

0926-3373/$ – see front matter © 2014 Elsevier B.V. All rights reserved.
http://dx.doi.org/10.1016/j.apcatb.2014.01.058

minerals [17,18], molecular sieves [19–21], transition metal oxides [13,22] and supported metal/metal oxides [23–25]. Red mud (RM) is an alkaline residue that is generated in large amounts during the extraction of aluminum from bauxite using the Bayer process [26]. The storage and maintenance of RM represents a significant environmental challenge to the aluminum industry because of the alkaline nature of this material and the risk that this possess to living organisms [26]. In general, RM is mainly composed of Fe, Al, Si and Ti oxides, as well as their oxyhydroxides and tectosilicate-like compounds [26]. Some of the main components of RM are widely used in water treatment processes, where they are used as coagulants [27,28], sorbents [29,30] and catalyst for the activation of peroxymonosulfate [31–33]. The use of RM in water treatment could provide an opportunity for turning into a valuable resource, as well as enhancing the socio-ecological-economic value of the aluminum industry. Furthermore, the Fe, Al, Si and Ti oxides and oxyhydroxides present in RM could be used in heterogeneous catalytic ozonation reactions as a catalyst or support. In additional, some other studies had found that cobalt oxides were active in heterogeneous catalytic ozonation [34,35]. Therefore, in this study, cobalt doped RM was used as a catalyst for the degradation of BZF in aqueous solution by ozonation. Main aims of this study were focused on (1) the evaluation of the catalyst in terms of its degradation performance; (2) the identification of any intermediates formed during the reaction and the elucidation of the reaction mechanism; and (3) the assessment of the toxicity of the RM in different oxidation processes.

2. Materials and methods

2.1. Chemicals and reagents

The RM samples used in the present study were obtained from China Shandong Hongqiao Aluminum Co., Ltd. (Shandong province, China) and were composed of particles in the range of 0.15–0.30 mm in size. The samples were washed with ultrapure water and air-dried prior to their use. BZF (>98% purity) was obtained from Sigma–Aldrich (USA). Ultrapure water (18.2 MΩ cm) was used throughout the current study and was obtained from a CLASSIC UVF pure water treatment system (ELGA Inc., UK). Acetonitrile and methanol (J.T. Baker Inc., USA) were degassed prior to being used for the high-performance liquid chromatography (HPLC) analyses performed as part of this study. All of the other reagents used in the current study were purchased as the analytical grade or higher, and were used without further purification. All of the glassware used in the current study was soaked in a $H_2SO_4/K_2Cr_2O_7$ solution overnight, before being washed sequentially several times with tap water and distilled water prior to its use.

2.2. Synthesis and characterization of cobalt doped RM

The cobalt doped RM catalyst, which shall be referred to as Co/RM hereafter, was prepared in our laboratory using a wetness impregnation method. Cobalt nitrate was used as the cobalt precursor because it underwent a better interaction with the supports than other cobalt precursors available for this process [31]. The fresh RM powder samples were washed with ultrapure water at least three times to remove any surface dust before being crushed and sieved to obtain particles of 0.15–0.3 mm in size. A portion of the resulting RM material (5.0 g) was then added to a solution of $Co(NO_3)_2{\cdot}6H_2O$ (1.022 g) in ultrapure water (100 mL), and the resulting suspension was stirred continuously at 333 K until all of the water had completely evaporated. The resulting residues were then collected and dried at 353 K overnight before being calcined at 673 K for 4 h in air. After the calcinations process, the samples were crushed and sieved to give particles of 0.15–0.3 mm in size before being stored in a desiccator prior to their use.

X-ray diffraction (XRD) patterns of the RM or Co/RM were collected on a Japan Rigaku D/max 12KW X-ray diffractometer using a filtered Cu Kα radiation source, with an accelerating voltage of 40 kV and a current of 30 mA, and scanned at 2θ from 5° to 80° at a rate of 4° min^{-1}. UV–visible diffuse reflectance spectra (UV–vis DRS) were recorded on a UV-365 (Shimadzu, Japan) equipped with an integrating sphere. $BaSO_4$ was used as a reference material and the wave was scanned from 300 to 800 nm.

The specific surface area and pore volume properties of the catalysts, including RM and Co/RM, were analyzed using an ASAP 2020M Surface Area and Porosity Analyzer (Micromeritics, USA). The level of N_2 gas adsorption–desorption was measures during this process at 77 K to obtain specific surface area information using the Brunauer–Emmett–Teller (BET) method, whereas the pore size distributions of the catalysts were determining by the Barrett–Joyner–Halenda (BJH) desorption dV/dlog(D) pore volume method. The total pore volume and the micropore were also calculated by this method. The mesopore was the total pore volume minus the micropore volume. The point of zero charges (pH_{PZC}) were determined using the method described previously by Altenor et al. [36]. Further details of this procedure are provided in the Supporting Information (SI, Text S1).

2.3. Catalytic ozonation procedure

A batch mode experiment was conducted at ambient temperature in a glass cylinder reactor with an effective solution volume of 250 mL to evaluate the degradation performances of the catalysts. Ozone was produced using a standard laboratory ozonizer (3S-A5, Beijing Tonglin Gaoke Technology, Beijing, China) supplied with the dry pure oxygen. After the generator had reached a steady state, ozone gas was bubbled into the ultrapure water in the reactor through a silica dispenser to give the desired dissolved ozone concentration under 297 K. This solution was used as a stock solution of dissolved ozone. A calculated volume of the dissolved ozone stock solution and the catalyst powder were then added to the BZF solution, with the magnetic stirrer being turned on at the same time. In this way, the ozone was introduced to the reaction system at once. Samples were collected from the reactor at specific time points and immediately quenched into an excess of a sodium sulfite solution (1.0 mM). Prior to their analysis, the samples were filtered with cellulose acetate filters (0.45 μm) to remove any catalyst particles. The cellulose acetate filters did not remove any of the BZF. To identify any of the intermediates formed during the different processes, a higher concentration of BZF (0.2 mM) was used in a continuous ozone gas purging mode experiment. In this mode, a constant dissolved ozone concentration of 0.38 mg/L was achieved with the diffuser at a flow rate of 1.0 mL/min, in the same glass cylinder reactor that was used in for the batch mode experiments. All of the experiments in the current study were conducted in triplicate and the standard deviations have been shown as error bars.

The dissolved BZF was analyzed by HPLC using a Waters2695 HPLC system (Waters, USA) equipped with a Waters2998 UV detector at a wavelength of 200 nm. The HPLC analyses were performed with an Agilent C18 column (150 mm × 4.6 mm, 5 μm, Agilent, USA) using an isocratic elution of 50% buffered solution ($H_2O/CH_3OH/H_3PO_4$ = 1000/25/0.002) and 50% CH_3CN at a flow rate of 1.0 mL/min. The intermediates were identified using a Finnigan SpectraSYSTEM® LC (Finnigan, USA) coupled with a Thermo Quest Finnigan LCQ Duo mass spectrometer system (Finnigan) equipped with an electrospray ionization interface operating in the electrospray ionization mode (LC–ESI/MS). The effluent (0.8 mL/min) was

delivered by a gradient system from a Thermo P4000 partitioned by the same column described before. The mobile phase consisted of a mixture of 0.1% formic acid (A) and an acetonitrile solution (B) containing 0.1% formic acid and 5% pure water, which was eluted according to the following gradient mode: (1) 95% A from 0 to 3 min; (2) from 3 to 53 min, B was increased in a linearly fashion from 5 to 60%, whereas A was simultaneously reduced to 40% and held for 2 min; and (3) from 55 to 59 min, the mobile phase was returned to its initial composition until the end of the run.

The dissolved ozone concentration was measured colorimetrically using the previously published indigo method [37], whereas the ozone gas type was measured using an iodometric method. The amount of Total Organic Carbon (TOC) was determined using a TOC-5000A Total Organic Carbon Analyzer (Shimadzu, Japan). The dissolution of ions during the reaction was analyzed by inductively coupled plasma–atomic emission spectrometry (ICP–AES, Optima 7000 DV, PerkinElmer, USA).

2.4. Toxicity assays

The unicellular green microalgae *Chlorella vulgaris* (*C. vulgaris*) was purchased from the Chinese Research Academy of Environmental Sciences and used to assay the algae toxicity according to the method previously described by Essam et al. [38]. Different types of solution were added individually to the algae growth medium (M-11) and care was taken to ensure that the final concentrations of the different solutions were the same. Following their inoculation with *C. vulgaris* that was in exponential phase, the test tubes were sealed with gauzes and cultured in artificial climate incubators (2000 lux, light:dark = 12 h:12 h and 298 ± 1 K). Growth was monitored periodically up to 96 h by measuring the algae cell concentration directly using an optical microscope (Chongqing Optec Instrument Co. Ltd, China). The inhibition test of *C. vulgaris* was calculated as follows:

$$I_y = \frac{Y_B - Y_A}{Y_B} \times 100\% \quad (1)$$

where Y_A and Y_B represent the average algae cell concentrations of three parallel *C. vulgaris* solutions and a blank solution without any oxidation, respectively, under the same culture conditions. The 96-EC_{50} values, which represent the effective concentrations required to provide 50% inhibition, were determined in 96-well plates.

3. Results and discussion

3.1. Performance and mineralization of ozonation, RM or Co/RM catalytic ozonation

Batch runs: the performances and mineralization of BZF in water are discussed below. The effectiveness profiles of the catalytic ozonation processes conducted in the presence of RM and Co/RM for the removal of BZF are shown in Fig. 1(A) as a batch mode experiment. The efficiency of the sole ozonation process for the removal of BZF was only 36.9%, and it would therefore not be possible to effectively remove the BZF using this contact time (30 min) in the sole ozonation process. We then proceeded to investigate the addition of RM or Co/RM to the process to enhance the removal efficiency (Fig. 1(A)). The efficiency of the catalytic ozonation process conducted in the presence of Co/RM for the removal of BZF reached 83.1%, whereas the efficiency only reached 64.0% when the ozonation process was conducted in the presence of RM. The addition of RM or Co/RM to the catalytic ozonation process led to an increase in the efficiency with which BZF could be removed from the water compared with the sole ozonation process. The degradation reactions in the catalytic ozonation process were complex because of the combination of the sole

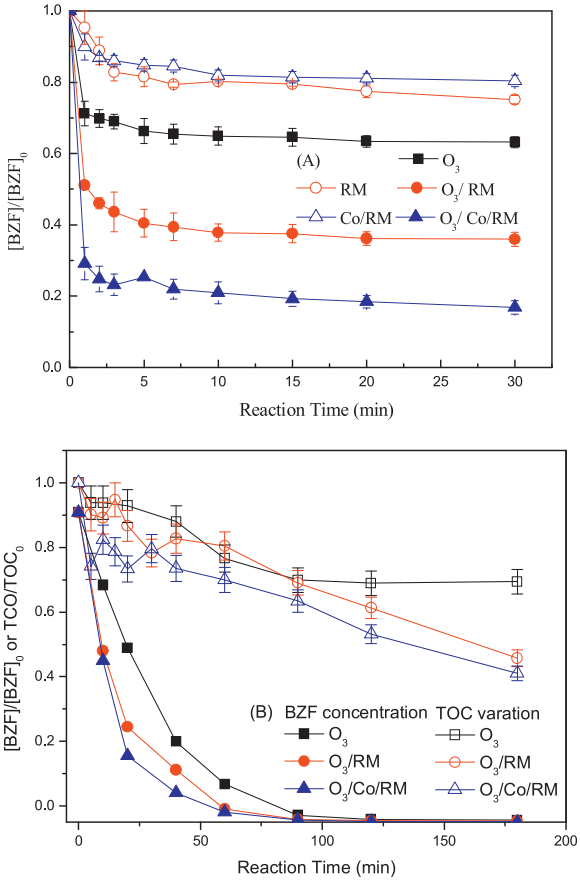

Fig. 1. Performance (A) and mineralization (B) of the sole ozonation and catalytic ozonation by RM and Co/RM. Reaction conditions: (A) batch ozonation, $[O_3]_0$ = 0.5 mg/L, $[BZF]_0$ = 2.76 μM [catalyst] = 50 mg/L, water pH 6.68; (B) continuous ozonation, $[O_3]_0$ = 0.38 mg/L, $[BZF]_0$ = 0.2 mM, [catalyst] = 1.0 g/L, water pH 6.68.

ozonation, catalytic reaction and adsorption processes, and it was therefore necessary to investigate the performances of the adsorption processes for the removal of BZF on the surfaces of the RM and Co/RM catalysts. The adsorption efficiencies of the RM and Co/RM catalysts for BZF were 24.9 and 19.6%, respectively. The removal efficiencies of the catalytic ozonation processes for BZF using the Co/RM catalysts were higher than the combined removal efficiency of the sole ozonation and surface adsorption processes, indicating that the Co/RM catalysts exhibited high levels of catalytic activity. However, RM showed a slight catalytic activity as the catalytic efficiency was only the combination by the sole ozonation and surface adsorption. Based on the adsorption and catalytic activity characteristics of the RM and Co/RM catalysts, the observed increases in the degradation rates of the catalytic ozonation reaction were attributed to (1) the generation of reactive oxygen species (ROS) during the catalytic ozonation; and (2) the adsorption of BZF onto the surface of catalyst, followed by the degradation of the absorbed BZF by ozone or ROS. The differences in the adsorption and catalytic activity properties of the RM and Co/RM catalysts were attributed to difference in their mineral composition and surface properties, which will be discussed in greater detail below.

Continuous runs: the performance profile for the degradation of BZF is shown in Fig. 1(B). In order to investigate the practical application, we also studied the Co/RM catalyst used for the wastewater treatment, the ozone was continuously bubbled through the reactor as opposed to being introduced as a single dose as described above. For the sole ozonation process with an ozone dosage of 0.36 mg/L, 95% of BZF was removed in 100 min,

although the initial concentration enlarged to 0.2 mM. The rapid degradation of the BZF under the sole ozonation condition was attributed to the ozone selectively attacking the conjugated aromatic rings/double bonds on the BZF molecule, with the electron donating amino group (–NH_2) effectively activating the aromatic ring by increasing its electronic density [39]. Furthermore, aromatic compounds such as BZF have highly delocalized electrons and exhibit enhanced reactivity towards ozone. The presence of RM or Co/RM could significantly increase the degradation rates in both cases, especially during the early stages of the process. Co/RM showed a higher catalytic activity than RM. The results verified that the reaction mechanism is not affected by the enlarging the initial BZF concentration. In addition, the mineralization profiles of the different processes were also compared. The total TOC decay in the catalytic ozonation after 180 min increased by 30.0%, compared with that in the sole ozonation (Fig. 1(B)). Furthermore, the use of Co/RM led to a more pronounced increase in the TOC degradation rate compared with RM. This enhancement of the TOC degradation suggested that the presence of RM or Co/RM could offer a quick and effective oxidation pathway involving ROS that would not only assist in the initial oxidation of BZF, but would also dominate the degradation of the resulting intermediates thereafter. This effect was more pronounced in the Co/RM catalytic ozonation process. In general, an increase in the amount of the active constituent favored an increase in the overall performance of the catalyst by providing an increase in the number of active sites, although this effect was limited, with excessive increases in the amount of active constituent having a negative effect [40,41]. This effect is known as the mature rule in heterogeneous AOPs. Also, the major aims of this study were to evaluate the performances of these catalysts, as well as characterizing their surfaces and structures and identifying any intermediates. With this in mind, we decided not to investigate the effect of the amount of cobalt doped onto the RM in any further detail. The effects of the ozone and the catalyst dosage on the catalytic ozonation, however are shown in Text S2 and Fig. S1.

3.2. Characterization of RM and Co/RM

The mineral composition, texture, structure and surface properties of the RM and Co/RM catalysts have been identified as important factors affecting their catalytic activity. Fig. 2(A) shows the XRD patterns of the RM and Co/RM catalysts. Hematite, goethite, quartz, muscovite and sodalite were identified as the major phases in the RM samples. The Co/RM catalyst showed different XRD patterns to the RM supports. For example, the amount of goethite was significantly reduced through decomposition during the high temperature calcination process to give hematite. In the Co/RM, hematite and quartz were identified as the major phases. Interestingly, however, no crystalline cobalt oxides were found in the Co/RM, likely because of low levels of Co doping or high levels of Co dispersion on the surface of the RM. Saputra et al. [31] also prepared Co oxides catalysts based on RM and found that no Co oxide peaks were observed by XRD analysis. The absence of Co oxide peaks in this particular case was attributed to the lower Co doping percentage (5.0 wt.%). Our XRD results concerning the lack of Co oxides in the modified RM were supported by the UV–vis DRS results shown in Fig. 2(B). RM showed a low intensity compared with Co/RM at 434 and 740 nm, where a migration of Co^{3+} ions to the octahedral position had occurred [42]. The Co^{2+} and Co^{3+} ions in the Co/RM gave two adsorption bands around 434 and 740 nm that were much stronger than those in the RM, proving the presence of CoO or Co_3O_4. This result confirmed that the decomposition of $Co(NO_3)_2$ in air would lead to the formation of Co_3O_4 under 673 K, which would ultimately lead to the observed greater catalytic activity of RM.

The N_2 gas adsorption–desorption isotherms of RM and Co/RM at 77 K are shown in Fig. 2(C), and the surface texture characteristics are listed in Table 1. Following the cobalt modification, the surface area increased significantly from 8 to 58 $m^2\ g^{-1}$, and there was also a significant increase in the total pore volume. Considerable changes in the pore structure were also observed (Fig. 2(D)), indicating that the roles of the micropore and mesopore were different in the RM and Co/RM. After cobalt modification, a decrease in the micropore volume was observed together with an increase in the mesopore volume. The latter of these effects was believed to be the main reason for the increase in the total pore volume. In general, the calcination process should lead to an increase in the specific surface area and result in the aggregation of particles, which would be confirmed by a reduction in the micropore volume [43]. Taken together, these results suggested that the formation of Co oxide on the RM led to the observed increase in the mesopore volume. However, this increasing did not develop the adsorption capacity. The pH_{PZC} and the net charge of BZF under this water pH also were the influence factor. Therefore, the development of the catalytic activity from RM to Co/RM may due to the cobalt modification.

Table 1 also shows the point of zero charge (pH_{PZC}) values of the RM and Co/RM. The pH_{PZC} value of the RM was decreased from 9.13 to 7.99 for the Co/RM following the Co doping process. Cobalt oxides are typically acidic oxides with pH_{PZC} values around 7.20. The mixing of the cobalt oxides with the RM (an alkaline pH_{PZC}), however, resulted in a change in the pH_{PZC} value. BZF has two pK_a values (i.e., $pK_{a,1}$ 3.83, $pK_{a,2}$ −0.84). BZF showed a negative charged status, under neutral pH conditions (pH 6.68) in water. In contrast, both the RM and Co/RM showed a positive status under the same reaction conditions, where $pH(6.68) < pH_{PZC}$. Charges of different polarity between BZF and the catalyst led to specific differences in the adsorption capacity. For less positive charges than RM, Co/RM exhibited a smaller adsorption capacity for BZF than RM. In terms of its resonance structure, ozone behaves as a Brønsted base because of its dipole [44]. Ozone may therefore react with the surface of solid metal oxide that exhibits strong Brønsted acidity, through the chemical adsorption of the ozone or ozone decomposition. Based on its pH_{PZC} value, Co/RM exhibited greater acidity than RM, and it was therefore speculated that the surface reaction between ozone and the surface of the catalyst would be stronger for Co/RM. This also provided a possible explanation for the higher level of catalytic activity observed for this catalyst.

3.3. Leaching of toxic heavy metals from RM or Co/RM during the catalytic ozonation

Based on the XRD results for the RM and Co/RM, there appeared to be some opportunity for the release of heavy metals from catalysts. Releases of this type could lead to three possible side effects, including (1) the leaching of toxic elements that could have an adverse impact on the aquatic environment and human health; (2) a reduction on the activity of the catalyst; and (3) the occurrence of a homogeneous catalytic ozonation that could further contribute to the removal of BZF. With this in mind, it was necessary to investigate the leaching of heavy metals into the solution during the catalytic ozonation process. The results for the composition of the RM and the Co/RM, as well as the leaching concentration in the catalytic ozonation are summarized in Table 2. The results for the composition of the RM and the Co/RM were consistent with the results from the XRD analysis. Fe and Al were found to be the main elements in both of the catalysts. Furthermore, no significant changes were observed in the metal composition, with the exception of cobalt in Co/RM after the cobalt doping process. The cobalt present in the Co/RM also confirmed the formation of cobalt oxides. After the catalytic ozonation conducted with the RM and

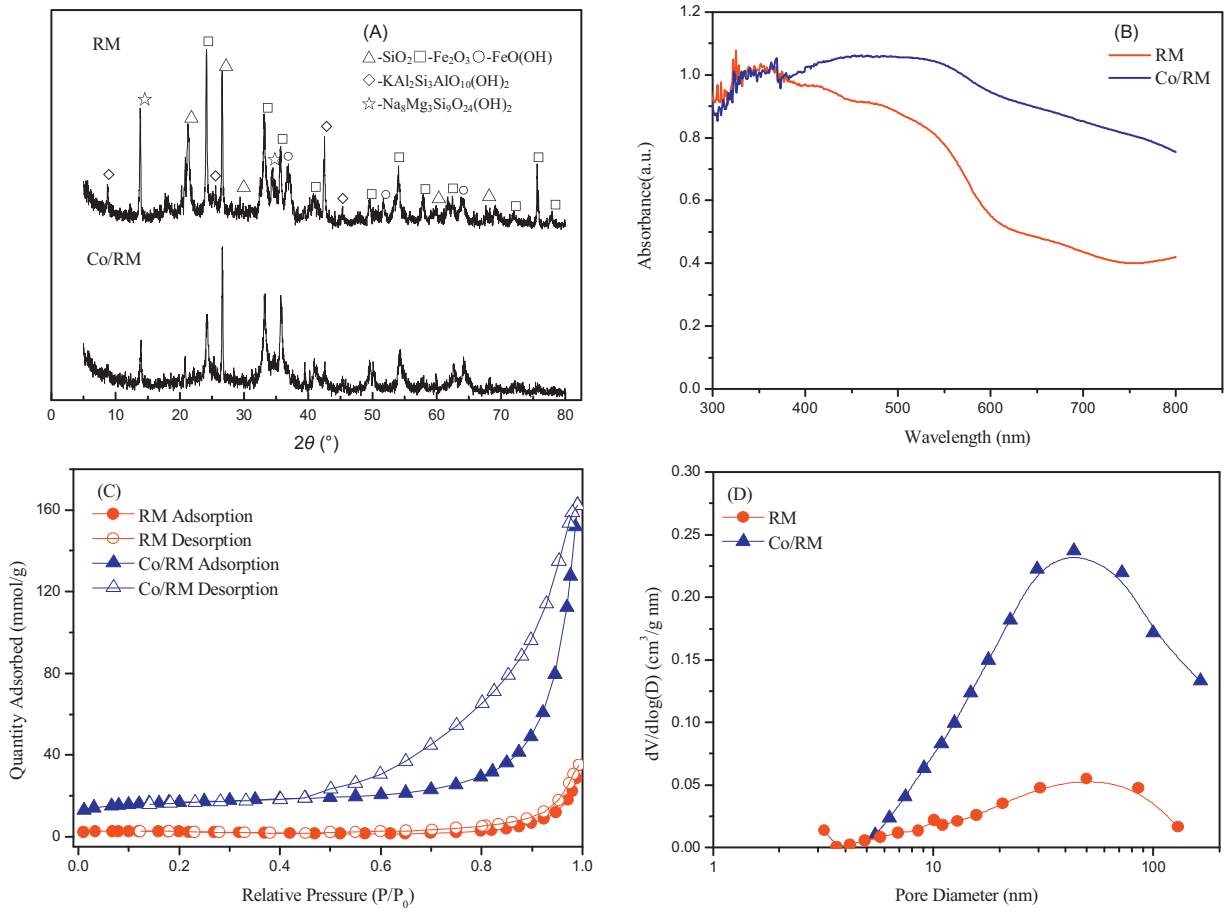

Fig. 2. Mineral composition, texture structure and surface properties of RM and Co/RM, (A) XRD spectrograms, (B) UV–vis DRS spectra; (C) Nitrogen adsorption–desorption isotherms, (D) BJH pore size distribution curves.

Table 1
Structure and surface properties of RM and Co/RM.

Catalyst	A_{BET}[a] ($m^2\ g^{-1}$)	V_{tot}[b] ($cm^3\ g^{-1}$)	V_{micro}[c] ($cm^3\ g^{-1}$)	V_{meso}[d] ($cm^3\ g^{-1}$)	D_{avg}[e] (nm)	pH_{PZC}
RM	8	3×10^{-2}	6×10^{-3}	2.4×10^{-2}	14.542	9.13
Co/RM	58	17×10^{-2}	1.5×10^{-3}	17.2×10^{-2}	12.100	7.99

[a] BET surface area.
[b] Total pore volume of the surface of catalyst.
[c] Micro pore volume of the surface of catalyst.
[d] Mesopore volume of the surface of catalyst.
[e] Average diameter of pore distributed over the surface of catalyst.

Co/RM catalysts, the metal elements in the solutions were found to be below the limits of detection. These results indicated that the two catalysts had released very little of their active elements into the solution through leaching. Based on results, these two catalysts therefore have the potential to be used safely in wastewater treatment processes. Furthermore, these observed low levels of metal leaching confirmed that the catalytic ozonation in this study were typical heterogeneous reaction, especially for Co/RM.

3.4. Reusability of the catalysts and their performance in a wastewater matrix

For the heterogeneous catalytic ozonation reactions using RM and Co/RM, it was essential to examine the catalytic efficiency of the spent/reused catalyst. The catalysts were reused four times to examine their performances for the degradation of BZF and the results are shown in Fig. 3(A). After each run, the catalyst was

Table 2
Leaching of toxicity heavy metal from RM or Co/RM in catalytic ozonation.

	Fe	Al	Co	Ca	Mg	Si
RM catalyst (mg/g)	175	100.5	ND	7.5	ND	0.675
Co/RM catalyst (mg/g)	178.5	106.5	44.4	7.48	ND	0.66
RM catalytic ozonation (mg/g)[a]	ND	ND	ND	ND	ND	ND
Co/RM catalytic ozonation (mg/g)[a]	ND	ND	ND	ND	ND	ND
Limit of detection (mg/L)	0.03	0.002	0.005	0.002	0.001	0.01

[a] Reaction condition: batch ozonation, $[O_3]_0 = 0.5$ mg/L, $[BZF]_0 = 2.76$ μM, [catalyst] = 50 mg/L, water pH 6.68, reaction time was 30 min.

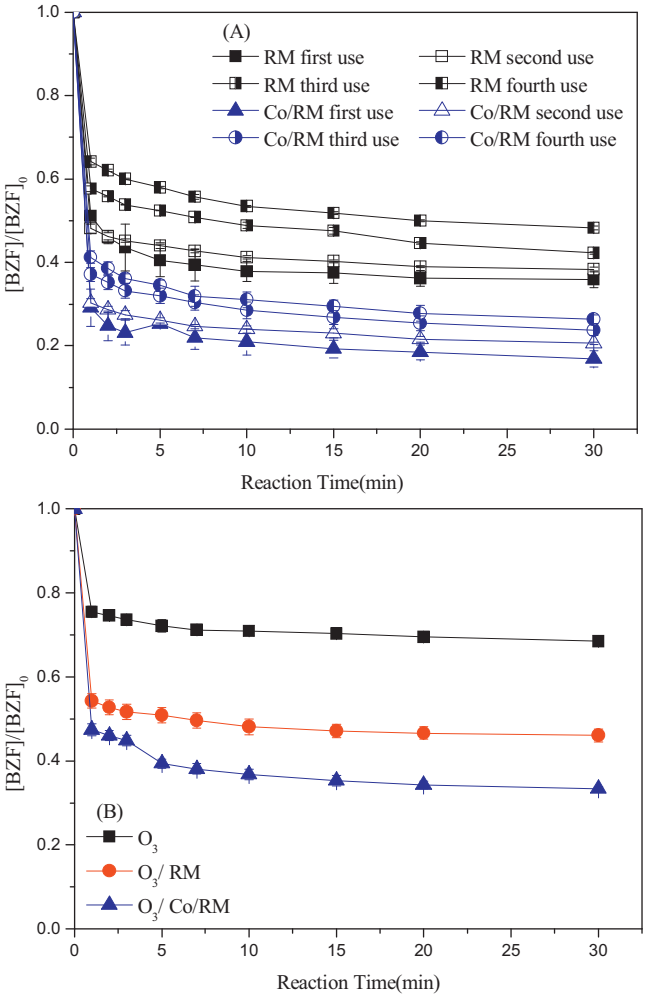

Fig. 3. (A) Reuse of the RM and Co/RM catalysts for the degradation of BZF, (B) Degradation performance of BZF in the effluent of domestic sewage. Reaction conditions: batch ozonation, $[BZF]_0 = 2.76\ \mu M$, [catalyst] = 50 mg/L, water pH 6.68; (A) $[O_3]_0 = 0.5$ mg/L; (B) $[O_3]_0 = 5.0$ mg/L.

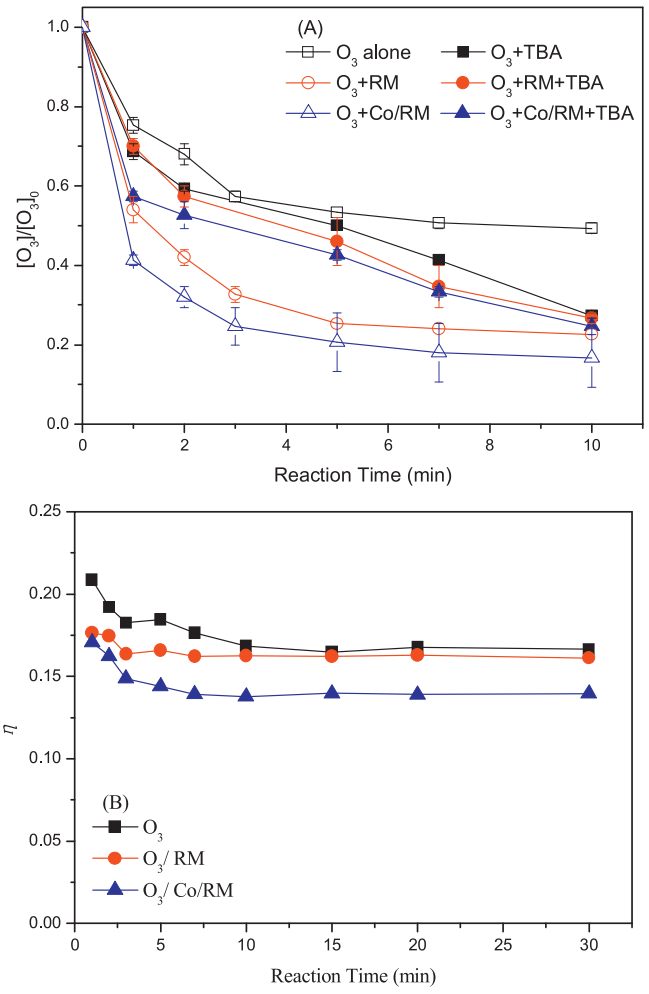

Fig. 4. (A) Catalytic ozone decomposition in the absence of BZF, (B) Ozone utilizing efficiency (η) in the degradation of BZF by the different processes. Reaction conditions: batch ozonation, $[O_3]_0 = 0.5$ mg/L, $[BZF]_0 = 2.76\ \mu M$, [catalyst] = 50 mg/L, [TBA] = 500 mg/L, water pH 6.68.

centrifuged, washed with ultrapure water, centrifuged again, and then dried at 70 °C. As expected, there was a small reduction of the performance after each run for both the RM and Co/RM, as noted from the slower initial decay rates and final removal efficiencies. This reduction in the performance was more pronounced for the RM catalysts, indicating that the doping of the surface of RM with Co oxide had led to an increase in the reusability performance of the catalyst. In practice, if a longer reaction time was adopted, a satisfactory value for the removal efficiency of BZF could always be obtained after each run. The accumulation of intermediates from the previous runs was suggested as a likely the reason for the observed reduction in the performance of the catalysts after each run [45]. These fixed intermediate would then compete with the BZF for ROS during the subsequent runs.

The decomposition profiles of BZF in the sole and catalytic ozonation reaction using RM and Co/RM were tested using the effluent from a wastewater treatment plant, and the water quality is shown in Table S1. To achieve better removal efficiency, the ozone dosage was increased to 5.0 mg/L. When domestic sewage effluent was used as a matrix, the removal efficiency in the sole ozonation was still very low, with a value of 31.5% after 30 min. Following the addition of RM and Co/RM catalysts, the removal efficiencies for BZF increased to 53.9% and 66.6%, respectively. The results shown in Fig. 3(B) implied that the two catalysts still showed catalytic activity in an actual body of water and that Co/RM still gave the best performance of the two catalysts. When a longer reaction time or higher dosage of catalyst was used, better removal efficiencies were achieved. These results also suggested that the two catalysts could potentially be used for the treatment of wastewater, especially the Co/RM catalyst.

3.5. Ozone variation in the sole ozonation and catalytic ozonations using RM and Co/RM

The ozone decomposition rates in the absence of BZF by the sole ozonation and RM or Co/RM catalyzed ozone ozonation were evaluated experimentally and the results are shown in Fig. 4(A). Molecular ozone was found to be unstable in water, which was confirmed by the decomposition of ozone during the sole ozonation to generate hydroxyl radical (•OH) [46]. The decomposition of ozone was therefore identified as the main reason for the indirect oxidation reaction (i.e., •OH reaction). The decomposition ability of ozone alone, however, was relatively weak, and the result revealed that the ozone self-decomposition efficiency was only 50.6% after 10 min under the neutral pH. RM appeared to enhance the rate of ozone decomposition, leading to a reduction in the aqueous ozone concentration of over 77.3% after 10 min. The increase in the performance of the BZF degradation in the RM catalytic ozonation was attributed to an increase in the rate of ozone decomposition

and the formation of more •OH. Co/RM exhibited an even greater rate of catalytic ozone decomposition (over 83.3% in 10 min). The order of ozone decomposition in these reaction processes was Co/RM > RM > ozone alone. This sequence was consistent with the efficiency of BZF degradation in these processes, indicating that the catalytic decomposition of ozone by RM and Co/RM was the main reaction pathway in terms of increasing the performance of BZF degradation. Fig. 4(A) also shows the effect of *tert*-butyl alcohol (TBA) on the (catalytic) ozone decomposition. TBA was used as an effective scavenger because of its stronger radical capturing ability, as indicated by its higher reaction rate constant with •OH, $k_{\bullet OH} = 6.0 \times 10^8$ L/(mol s). Furthermore, TBA reacted with molecular ozone with a lower reaction constant of $k_{O_3} = 3.0 \times 10^{-3}$ L/(mol s) [40]. Another reason for the selection of TBA as the quencher was its low level of adsorption onto the solid surface [47]. In the sole ozone decomposition, the ozone self-decomposition efficiency was only 50.6% after 10 min under the neutral pH. When TBA was added into the sole ozone decomposition system, a small increase in the rate of ozone decomposition was observed. The self-decomposition efficiency of the ozone was 72.6% around the same reaction time. To the best of our knowledge, this result has never before been reported in the batch experiment mode. Under these aqueous conditions, the molecule ozone and •OH generated from the decomposition of ozone would exist in solution. The TBA would then react with and ultimately consume the molecule ozone. This small increase in the rate of decomposition therefore indicated that molecule ozone was present and did not decompose completely under these aqueous conditions. The presence of TBA inhibited the reactions involving RM and Co/RM, confirming that the catalytic decomposition of ozone generated •OH. The ozone decomposition efficiencies of the different processes in the presence of TBA were ultimately all the same, indicating that the TBA concentration used was sufficient to inhibit the formation of •OH. The results of these TBA inhibition experiments suggested that the addition of the catalysts generated more •OH, which led to an enhancement in the degradation performance compared with the sole ozone reaction. The inhibitory effect on the Co/RM process was greater than that in the RM process, indicating that more •OH was generated in the Co/RM process. The catalytic decomposition of ozone to generate •OH was therefore identified as the main reason for the observed better performance of Co/RM in the degradation of BZF compared with RM or the sole ozonation processes.

Fig. 4(B) shows the corresponding effective ozone consumption ratio (η) during the sole ozonation and catalytic ozonation processes involving RM and Co/RM. The index η was defined as following:

$$\eta = \frac{[BZF]_0 - [BZF]_t}{[O_3]_0 - [O_3]_t} \quad (2)$$

where $[BZF]_0$ and $[BZF]_t$ are the concentrations of BZF in the solution at the beginning of the reaction and at a later reaction time (t), respectively, and $[O_3]_0$ and $[O_3]_t$ are the concentrations of aqueous dissolved ozone in the solution at the beginning of the reaction or at a later reaction time (t), respectively. Based on Eq. (2), it is clear that the higher the value of η, the higher the effective molecule ozone consumption. A specific tendency was observed in all of the reaction process, in that as the reactions proceeded, η decreased sharply during the first 10 min and gradually moved towards a plateau. This experiment phenomenon indicated that the molecular ozone was being consumed almost entirely during the first 10 min of the reaction in all of the different reaction processes. The molecular ozone would decompose to •OH during the initial phases of both the sole and catalytic ozonation reactions. The variation of η was reduced following the addition of the catalysts. In the Co/RM catalytic ozonation, η exhibited the lowest effective ozone consumption. The η value in the RM catalytic ozonation was more than that of the Co/RM process, but lower than that of the sole ozonation. In our study, the aqueous ozone was consumed through a combination of direct and indirect oxidation processes, under this water pH. Based on the results in Fig. 4(A) and (B), the presence of RM and Co/RM clearly led to an increase in the decomposition of ozone, and it was therefore concluded that the lower η value in the catalytic ozonation was caused by the ozone decomposition process and the degradation of BZF during the catalytic ozonation and was dominated by the •OH oxidation rather than the molecule ozone reaction.

3.6. Intermediates and reaction pathways of BZF in the different processes

To identify the intermediates resulting from the degradation of BZF in the sole ozonation and catalytic ozonation reactions involving RM or Co/RM, the initial concentration of BZF was increased to 0.2 mM to provide a better resolution in the LC–ESI/MS, and this concentration was also used to study the evolution of intermediates by LC (UV detector). The sole ozonation in this study was conducted at a pH of 6.68 without TBA, and it was therefore envisaged that the reaction would involve a combination of molecular ozone and •OH oxidation. The introduction of a catalyst (i.e., RM or Co/RM) led to an increase in the formation of •OH (Fig. 4) and 22 identical intermediates were detected in the sole ozonation and catalytic ozonation reactions. A summary of the identified intermediates is shown in Table S2, and the ESI/MS data for the different compounds are shown in Fig. S2. Among the 22 intermediates, there were 7 isomers that could be arranged into three groups (i.e., compounds C13 and C14, C16 and C18, and C19, C20 and C22). The process involved in the identification of these isomeric intermediates is described in Text S3.

Based on the identities of these different intermediates (Fig. S2), as well as their yields in the sole ozonation (Fig. S3) and catalytic ozonation (Figs. S4 and S5), we have proposed pathway for the degradation of the BZF during these reactions, which is shown in Fig. 5. Dantas et al. [9] reported that there were two sites in BZF that could be attacked by molecule ozone. In this study, the process of identifying the intermediates was performed in the absence of TBA, and the number of potential attack sites was increased to four (Fig. 5) because of the co-contributions of molecule ozone and •OH. Sites 1 or 3 could be two possibilities for the oxidation of the 4-chlorobenzoly ring or the phenoxy moiety. A variety of hydroxylated intermediates were detected during the course of this study, with the hydroxylation on the benzene ring occurring in a stepwise manner. Detailed information of this type concerning the intermediates resulting from BZF has never been reported before in publications involving the ozonation [9] or catalytic ozonation [10] of BZF, although similar information has been reported in a typical •OH reaction involving a TiO_2 photocatalytic processes [5]. The monohydroxylated intermediates identified during the course of this study were characterized by an increasing of 16 Da in m/z value from that of the parent BZF (m/z 362 in positive), and subsequently named as C18 (attack on the phenoxy ring, named as Pathway A) and C16 (attacked on the chlorine-containing ring, named as Pathway B). Compounds such as C16 and C18 correspond to the addition one •OH to the parent BZF. In this step, the hydroxylation was facilitated by the *ortho* and *meta* orientation in either the chlorine-containing or the phenoxy ring. Based on the LC-MS spectra, none of the other isomers were formed. It was envisaged that the *meta*-hydroxylated intermediate would be formed via a minor pathway because of the steric effect of the bulky –O–R and –Cl groups [48,49]. The advanced oxidation on the benzene ring could lead to the formation of poly-hydroxylated intermediates, such as C20, which was identified by Dantas et al. [9] and C22. The –Cl group had a deactivating effect on the benzene ring [50]. An increase in the oxidation

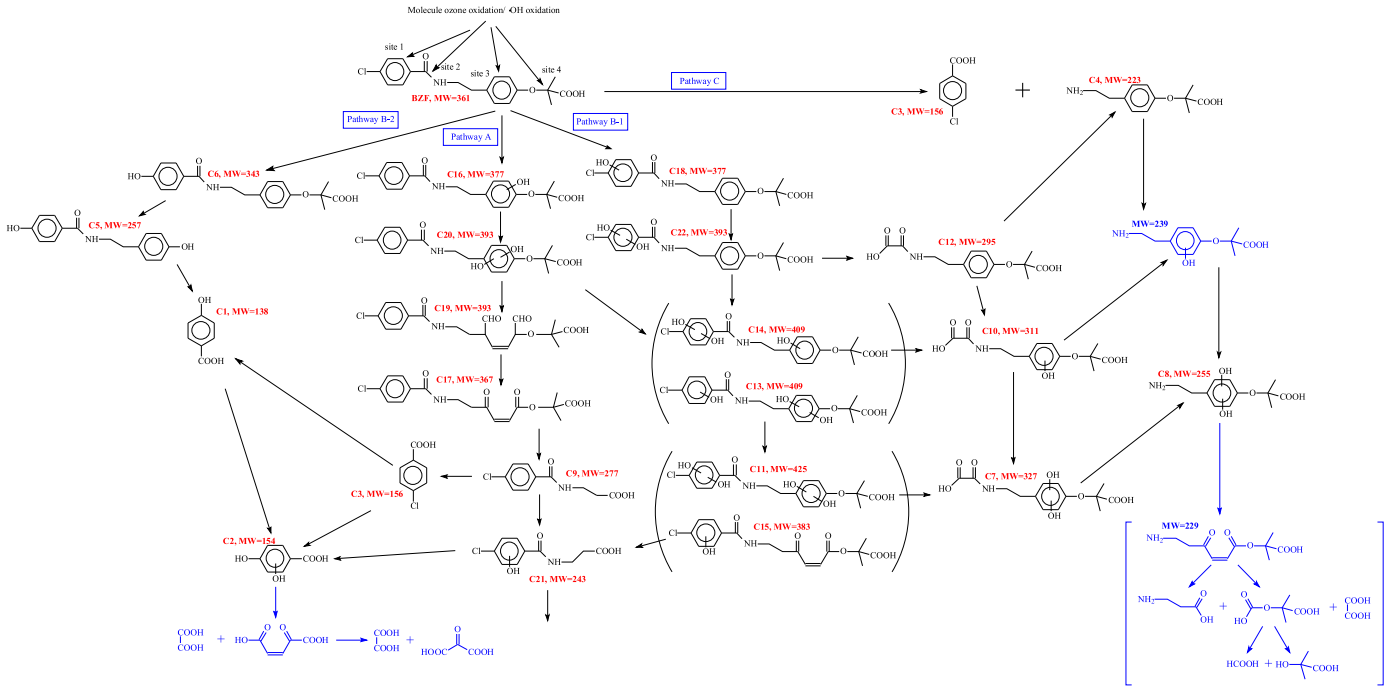

Fig. 5. Pathway of BZF degradation in the catalytic ozonation processes, the non-proposed intermediates are shown in parentheses.

energy (dosage or reaction time) was needed to break out this ring, which resulted in similar phenomenon in pathways A and B. The continuous oxidation of C20 and C22 could lead to hydroxylation substitute (C14) or the cleavage of the aryloxy-carbon bond on the phenoxy ring (C19), which would lead to the opening of this ring (C17 and C9). Following the opening of the phenoxy ring, hydroxylation was also observed on the chlorine-containing ring, as in the monohydroxylated product (C21) and the poly-hydroxylated product (C2). The amino group (–NH–) in C9 was also attacked to generate C3, which has been reported previously as an intermediate in ozonation and catalytic ozonation [10]. Some small molecule organic acids (SMOAs) were also generated from C2 as the final products. This route was denoted as Pathway A. Further hydroxylation on the chlorine-containing ring of C14 would lead to ring opened products, such as C7, C10 and C12. The stepwise hydroxylation of the phenoxy ring was also observed in these products, resulted in the opening of the chlorine-containing ring. After that, the other benzene ring would be attacked step by step to generate SMOAs. This route was denoted as Pathway B-1. During the oxidation process of the chlorine-containing ring, the Cl would be directly substituted by an –OH group to give products C6 and C5. Being different from Pathway A and Pathway B-1, the stepwise hydroxylation of the benzene rings of C6 and C5 was not observed. This route was denoted as Pathway B-2. Sites 2 and 4 could be achieved by the attack of active sites such as –NH– or –O–R, to give uniform electron density distributions. The presence of C3 and C4 confirmed this hypothesis, and the pathway was denoted as Pathway C. In contrast to other reports, the occurrence of a reaction involving the hydroxyl-substitution of the –O–R moiety on BZF was not detected in this study.

Based on the profiles of the intermediates generated during the sole ozonation and catalytic ozonation (Figs. S3–S5) reactions, it was possible to identify the primary reaction pathways of the different processes. In the sole ozonation, the yields of C18, C20 and C22 were higher than those of the other products containing two benzene rings, indicating that Pathways A and B-1 were the main degradation pathways. The yields of C9 and C19 in Pathway A were significant higher than those of the other products containing one benzene ring from Pathway B-1, and it was therefore confirmed that Pathway A dominated the fate of BZF in the sole ozonation reaction.

The catalytic ozonation reactions with RM and Co/RM enhanced the mineralization of BZF, as shown in Fig. 1(B). These results were verified on the basis of the intermediate profiles. In the RM catalytic ozonation reaction, the yields of the products containing a benzene ring were lower than those observed in the sole ozonation reaction. The concentrations of C18 and C20 were much higher than those of the other products containing two benzene rings, indicating that Pathway A was the main route in this particular process. This conclusion was also supported by the products for the products containing one benzene ring. The concentrations of C9 and C19 in the catalytic ozonation using RM were lower than the concentrations found in the sole ozonation reaction. Importantly, the yield of C1 was much higher than that observed in the sole ozonation reaction. These variations indicated that the presence of RM enhanced the oxidative capacity of the system. When the RM was modified with Co oxides, the oxidation capacity was enhanced significantly to give C1, C9 and C18 as the critical intermediates. The concentrations C9 and C18 were decreased in the Co/RM catalytic ozonation reaction, although these were only minor reductions compared with RM catalytic process. The concentration of C1 in the Co/RM catalytic ozonation was reduced only slightly to begin with, but there was a steep drop after 120 min of the reaction, indicating that ring opening reactions could be achieved in the Co/RM catalytic ozonation.

To evaluate the pattern of intermediates between the different reaction processes, we considered the variations in the concentrations of the intermediates with one or two benzene rings in the different oxidation processes, as shown in Fig. 6. In all processes, the yields of the intermediates with one benzene ring were higher than those of the intermediates with two rings, indicating that ozone could attack the benzene ring of BZF as well as the corresponding products with two rings. In the sole ozonation, there was a peak (40 min) corresponding to intermediates with two benzene rings. However, this peak was not observed in the catalytic ozonation reactions involving RM and Co/RM. For intermediates with one

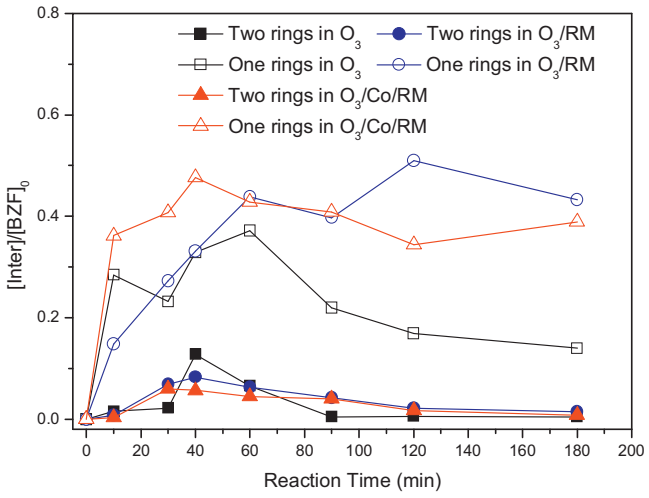

Fig. 6. Variation in the different types of intermediates during the different processes. Reaction conditions: continuous ozonation, $[O_3]_0$ = 0.38 mg/L, $[BZF]_0$ = 0.2 mM, [catalyst] = 1.0 g/L, water pH 6.68.

ring, significant differences were observed between these different reaction processes. The yields in the sole ozonation were found to be the lowest and increased in the catalytic ozonation reactions. In the Co/RM catalytic ozonation, the yields increased and decreased more quickly than they did in the RM catalytic ozonation reaction, indicating the stronger capacities of the oxidation and mineralization processes in the Co/RM reaction. In other studies, they had found the production of small molecule weight organic acids [10] that was not investigated in our study. In our study, C1 was found in the highest concentration of all of the products with one benzene ring, indicating that C1 was the final product in this study.

3.7. Toxicity assessment of the different degradation processes

Toxicological tests were conducted on a solution of BZF either without oxidation or that had been subjected to the sole ozonation or catalytic ozonation processes involving RM and Co/RM, and were based on the measurement of the inhibition of the growth of *C. vulgaris*, shown in Table 3. The toxicity assessment for a 96 h-EC_{50} of BZF without any oxidation was 40.2%. After the sole ozonation process, the 96 h-EC_{50} value increased to 50.5%. This increase in the 96 h-EC_{50} value indicated a decrease in the toxicity, suggesting that the sole ozonation process led to a reduction in the toxicity of BZF in the solution, even though it did provide a high level of BZF degradation. The poor removal efficiency and mineralization of the sole ozonation process lead to lower levels of BZF degradation and the generation of intermediates. A reduction in the toxicity was therefore observed in this study. After the addition of RM, the toxicity increased slightly from 40.2 to 43.0%. There were two possible reasons for this result, including (1) the higher removal efficiency of BZF during the RM catalyzed ozonation could have led to the formation of intermediates that could increase the toxicity; and (2) the RM could release alkalinity or toxic heavy metal ions (negated by Table 2) into the solution that could inhibit the growth of *C. vulgaris*. An interesting result was obtained for the Co/RM catalyzed ozonation reaction, where the 96-EC_{50} value was found to be 63.0% and therefore much higher than that observed from the others process, showing that the solution was relatively safe to the environment following the Co/RM catalytic ozonation. The catalytic ozonation by Co/RM did not only lead to an increase in the removal efficiency, but also led to differences in the profile of the intermediates. On the basis of these results, it was clear that the Co modified method was not only successful in providing enhanced levels of BZF removal and mineralization during the catalytic ozonation, but also led to a reduction in the toxicity of the solution after the catalytic cycle.

4. Conclusion

In the current study, red mud (RM) and cobalt doped red mud (Co/RM) were investigated as catalysts for the removal and mineralization of bezafibrate (BZF) solutions by catalytic ozonation. The primary intermediates resulting from these reaction processes were also identified and the toxicities associated with the different processes were evaluated.

(1) The sole ozonation did not allow for the effective removal of BZF. After the addition of RM and Co/RM, the performances of the ozonation reactions with regards to the BZF and mineralization processes were improved to different degrees based on the generation of hydroxyl radical (•OH). Both the fresh and reused Co/RM showed better catalytic activities than the RM in terms of BZF removal. These results were also observed in a matrix composed of domestic sewage effluent.
(2) The degradation pathways of BZF in both processes have been studied in detail with 22 primary intermediates identified. The catalytic ozonation reactions with RM and Co/RM resulted in the attack of the benzene ring of BZF and led to significant changes in the profiles of the intermediates. Co/RM showed much stronger catalytic activity than RM in terms of the ring opening reactions of the aromatic groups in BZF.
(3) The Co/RM catalyst provided the best performance of the two catalysts in terms of the removal of BZF from the effluent matrix, lower levels of leaching of toxic metal ions and a reduction in the toxicity of *C. vulgaris* following the Co/RM catalytic ozonation, indicating that Co/RM was an effective catalyst for the removal and detoxification of BZF from aqueous solutions.

Acknowledgements

This work was carried out with the support of the National Natural Science Foundation of China (nos. 51378063, 51108030 and 41273137), Beijing Natural Science Foundation (no. 8132033),

Table 3
Toxicity assessment of different degradation process by *Chlorella vulgaris*.

BZF alone		Ozonation		RM catalytic ozonation		Co/RM catalytic ozonation	
Percentage concentration (v/v, %)	Inhibition (%)	Percentage concentration (v/v, %)	Inhibition (%)	Percentage concentration (v/v, %)	Inhibition (%)	Percentage concentration (v/v, %)	Inhibition (%)
0	0	0	0	0	0	0	0
20	31.7	20	33.4	20	34.9	20	16.2
30	40	40	47.5	40	47	40	30.4
40	46.3	60	59.8	60	74.8	60	46.5
50	57	80	68.6	80	77.7	80	64.7
96 h-EC_{50} = 40.2%		96 h-EC_{50} = 50.5%		96 h-EC_{50} = 43.0%		96 h-EC_{50} = 63.0%	

Reaction condition: batch ozonation, $[O_3]_0$ = 0.5 mg/L, $[BZF]_0$ = 2.76 μM, [catalyst] = 50 mg/L, water pH 6.68, reaction time was 30 min.

the Specialized Research Fund for the Doctoral Program of Higher Education (no. 20100014120001), China Post Doctoral Science Foundation (nos. 201104060 and 2012M520006) and Open Project of State Key Laboratory of Urban Water Resource and Environment, Harbin Institute of Technology (nos. ES201204 and QAK201306).

Appendix A. Supplementary data

Supplementary material related to this article can be found, in the online version, at http://dx.doi.org/10.1016/j.apcatb.2014.01.058.

References

[1] D.W. Kolpin, E.T. Furlong, M.T. Meyer, E.M. Thurman, S.D. Zaugg, L.B. Barber, H.T. Buxton, Environ. Sci. Technol. 36 (2002) 1202–1211.
[2] M. Cleuvers, Ecotoxicol. Environ. Saf. 59 (2004) 309–315.
[3] N. Nakada, H. Shinohara, A. Murata, K. Kiri, S. Managaki, N. Sato, H. Takada, Water Res. 41 (2007) 4373–4382.
[4] B. Yang, G.G. Ying, J.L. Zhao, S. Liu, L.J. Zhou, F. Chen, Water Res. 46 (2012) 2194–2204.
[5] D.A. Lambropoulou, M.D. Hemando, I.K. Konstantinou, E.M. Thurman, I. Ferrer, T.A. Albanis, A.R. Fernandez-Alba, J. Chromatogr. A 1183 (2008) 38–48.
[6] H. Yuan, Y.L. Zhang, X.F. Zhou, Clean-Soil Air Water 40 (2012) 239–245.
[7] M. Isidori, A. Nardelli, L. Pascarella, M. Rubino, A. Parrella, Environ. Int. 33 (2007) 635–641.
[8] J.E. Drewes, T. Heberer, K. Reddersen, Water Sci. Technol. 46 (2002) 73–80.
[9] R.F. Dantas, M. Canterino, R. Marotta, C. Sansa, S. Esplugas, R. Andreozzi, Water Res. 41 (2007) 2525–2532.
[10] A. Goncalves, J.J.M. Orfao, M.F.R. Pereira, Appl. Catal. B 140 (2013) 82–91.
[11] B. Razavi, W.H. Song, W.J. Cooper, J. Greaves, J. Jeong, J. Phys. Chem. A 113 (2009) 1287–1294.
[12] A.G. Trovo, S.A.S. Melo, R.F.P. Nogueira, J. Photochem. Photobiol. A 198 (2008) 215–220.
[13] S. Song, Z.W. Liu, Z.Q. He, A.L. Zhang, J.M. Chen, Environ. Sci. Technol. 44 (2010) 3913–3918.
[14] T. Zhang, W.W. Li, J.P. Croue, Environ. Sci. Technol. 45 (2011) 9339–9346.
[15] J.R. Kastner, R. Ganagavaram, P. Kolar, A. Teja, C.B. Xu, Environ. Sci. Technol. 42 (2008) 556–562.
[16] C.A. Orge, J.J.M. Orfao, M.F.R. Pereira, Appl. Catal. B 126 (2012) 22–28.
[17] F. Qi, B.B. Xu, Z.L. Chen, J. Ma, D.Z. Sun, L.Q. Zhang, F.C. Wu, J. Hazard. Mater. 168 (2009) 246–252.
[18] F. Qi, Z.L. Chen, B.B. Xu, Z.Z. Xu, J. Water Supply Res. Technol. 57 (2008) 427–434.
[19] C.W. Kwong, C.Y.H. Chao, K.S. Hui, M.P. Wan, Environ. Sci. Technol. 42 (2008) 8504–8509.
[20] A. Ikhlaq, D.R. Brown, B. Kasprzyk-Hordern, Appl. Catal. B 123 (2012) 94–106.
[21] A. Ikhlaq, D.R. Brown, B. Kasprzyk-Hordern, Appl. Catal. B 129 (2013) 437–449.
[22] A.H. Lv, C. Hu, Y.L. Nie, J.H. Qu, Appl. Catal. B 117 (2012) 246–252.
[23] L. Zhao, Z.Z. Sun, J. Ma, Environ. Sci. Technol. 43 (2009) 4157–4163.
[24] L. Zhao, Z.Z. Sun, J. Ma, H.L. Liu, Environ. Sci. Technol. 43 (2009) 2047–2053.
[25] T. Zhang, W.W. Li, J.P. Croue, Appl. Catal. B 121 (2012) 88–94.
[26] S.B. Wang, H.M. Ang, M.O. Tade, Chemosphere 72 (2008) 1621–1635.
[27] E. Poulin, J.F. Blais, G. Mercier, Hydrometallurgy 92 (2008) 16–25.
[28] J. Fu, Y.H. Ding, G.Y. Ma, J. Yang, Q.F. Zeng, M.Y. Liu, D.S. Xia, H.L. Zhu, S.Q. An, Ozone-Sci. Eng. 31 (2009) 294–300.
[29] S. Vasudevan, J. Lakshmi, G. Sozhan, Environ. Sci. Pollut. Res. 19 (2012) 2734–2744.
[30] Y.Q. Zhao, Q.Y. Yue, Q.A. Li, B.Y. Gao, S.X. Han, H. Yu, J. Hazard. Mater. 182 (2010) 309–316.
[31] E. Saputra, S. Muhammad, H.Q. Sun, H.M. Ang, M.O. Tade, S.B. Wang, Catal. Today 190 (2012) 68–72.
[32] R.C.C. Costa, F.C.C. Moura, P.E.F. Oliveira, F. Magalhaes, J.D. Ardisson, R.M. Lago, Chemosphere 78 (2010) 1116–1120.
[33] S. Muhammad, E. Saputra, H.Q. Sun, H.M. Ang, M.O. Tade, S.B. Wang, Ind. Eng. Chem. Res. 51 (2012) 15351–15359.
[34] P.M. Álvarez, F.J. Beltrán, J.P. Pocostales, F.J. Masa, Appl. Catal. B 72 (2007) 322–330.
[35] P.C.C. Faria, D.C.M. Monteiro, J.J.M. Órfão, M.F.R. Pereira, Chemosphere 74 (2009) 818–824.
[36] S. Altenor, B. Carene, E. Emmanuel, J. Lambert, J.J. Ehrhardt, S. Gaspard, J. Hazard. Mater. 165 (2009) 1029–1039.
[37] H. Bader, J. Hoigne, Water Res. 15 (1981) 449–456.
[38] T. Essam, M. Aly Amin, O. El Tayeb, B. Mattiasson, B. Guieysse, Water Res. 41 (2007) 1697–1704.
[39] A.G. Gonçalves, J.J.M. Órfão, M.F.R. Pereira, J. Hazard. Mater 239–240 (2012) 167–174.
[40] J. Bing, L. Li, B. Lan, G. Liao, J. Zeng, Q. Zhang, X. Li, Appl. Catal. B 115–116 (2012) 16–24.
[41] R. Huang, H. Yan, L. Li, D. Deng, Y. Shu, Q. Zhang, Appl. Catal. B 106 (2011) 264–271.
[42] G.A.H. Mekhemer, H.M.M. Abd-Allah, S.A.A. Mansour, Colloid Surf. A 160 (1999) 251–259.
[43] F. Qi, B.B. Xu, L. Zhao, Z.L. Chen, L.Q. Zhang, D.Z. Sun, J. Ma, Appl. Catal. B 121 (2012) 171–181.
[44] F. Qi, B. Xu, Z. Chen, J. Ma, D. Sun, L. Zhang, Sep. Purif. Technol. 66 (2009) 405–410.
[45] F. Qi, W. Chu, B. Xu, Appl. Catal., B 134–135 (2013) 324–332.
[46] F. Qi, Z. Chen, B. Xu, J. Shen, J. Ma, C. Joll, A. Heitz, Appl. Catal. B 84 (2008) 684–690.
[47] M. Sui, J. Liu, L. Sheng, Appl. Catal. B 106 (2011) 195–203.
[48] K.L. Mardis, A.J. Glemza, B.J. Brune, G.F. Payne, M.K. Gilson, J. Phys. Chem. B 103 (1999) 9879–9887.
[49] E. Dorrestijn, P. Mulder, J. Chem. Soc. Perkin Trans. 2 (1999) 777–780.
[50] M.M. Huber, S. Canonica, G.-Y. Park, U. von Gunten, Environ. Sci. Technol. 37 (2003) 1016–1024.